



**HAL**  
open science

## Compression zone with partial stiffeners in beam-to-column steel connections

Sabra Bougoffa, Omar Mezghanni, Sébastien Durif, Abdelhamid Bouchaïr,  
Atef Daoud

► **To cite this version:**

Sabra Bougoffa, Omar Mezghanni, Sébastien Durif, Abdelhamid Bouchaïr, Atef Daoud. Compression zone with partial stiffeners in beam-to-column steel connections. *Engineering Structures*, 2021, 229, pp.111674 -. 10.1016/j.engstruct.2020.111674 . hal-03493155

**HAL Id: hal-03493155**

**<https://hal.science/hal-03493155>**

Submitted on 2 Jan 2023

**HAL** is a multi-disciplinary open access archive for the deposit and dissemination of scientific research documents, whether they are published or not. The documents may come from teaching and research institutions in France or abroad, or from public or private research centers.

L'archive ouverte pluridisciplinaire **HAL**, est destinée au dépôt et à la diffusion de documents scientifiques de niveau recherche, publiés ou non, émanant des établissements d'enseignement et de recherche français ou étrangers, des laboratoires publics ou privés.



Distributed under a Creative Commons Attribution - NonCommercial 4.0 International License

# Compression zone with partial stiffeners in beam-to-column steel connections

Sabra BOUGOFFA <sup>a,b,\*</sup>, Omar MEZGHANNI <sup>b,c</sup>, Sébastien DURIF <sup>a</sup>, Abdelhamid BOUCHAÏR <sup>a</sup>, Atef DAOUD <sup>b,c</sup>

<sup>a</sup> *Université Clermont Auvergne, CNRS, SIGMA Clermont, Institut Pascal, F-63000 Clermont-Ferrand, France.*

<sup>b</sup> *Université de Tunis El Manar, Ecole Nationale d'Ingénieurs de Tunis, LGC, BP 37, le Belvédère, 1002 Tunis, Tunisie.*

<sup>c</sup> *Université de Sfax, Ecole Nationale d'Ingénieur de Sfax, Département de Génie Civil, Route de Soukra Km 3,5, BP 1173,3038, Sfax, Tunisie.*

**Abstract:** The compression zone in beam-to-column connection can generally imply the use of transverse stiffeners. This paper presents the results of experimental tests to evaluate the strength of steel panels with various transverse stiffener configurations under concentrated load. These results are used to validate the developed finite element models. Twelve panels made of either hot rolled I-sections or welded I-sections have been tested. Different transverse stiffeners are studied including single sided, double sided and partial stiffeners. The main observed results are the maximum strength and the failure mode. The results of the experimental tests are compared with those given by the finite element model using shell elements. The comparison makes it possible to calibrate the nonlinear model considering the elastic-plastic behavior of materials and large displacements. Furthermore, the results are compared with existing analytical formulas for unstiffened and fully stiffened panels to evaluate their accuracy.

**Key-words:** transverse stiffeners, finite element, experimental tests, beam-to-column connection

\*Corresponding author.

E-mail addresses: [sabra.bougoffa@etu.uca.fr](mailto:sabra.bougoffa@etu.uca.fr), (S. Bougoffa), [omar.mezghannir@enis.tn](mailto:omar.mezghannir@enis.tn), (O. Mezghanni), [sebastien.durif@uca.fr](mailto:sebastien.durif@uca.fr), (S. Durif), [abdelhamid.bouchair@uca.fr](mailto:abdelhamid.bouchair@uca.fr), (A. Bouchair), [atef.daoud@enis.tn](mailto:atef.daoud@enis.tn), (A. Daoud)

## 1. Introduction:

Welds and bolts [1] are mainly used in beam-to-beam, column-to-column and beam-to-column connections. Beam-to-column connection can be single-sided or double-sided with various dimensions of beams [2,3]. According to EN1993-1-8 [1], beam-to-column connection transferring bending moment can be analyzed considering tensile zone, compression zone and shear zone. The behavior of each component is defined, and all the components are combined to obtain that of the whole connection. In last decades, numerous numerical and experimental studies focused on the behavior of the tensile zones in the beam-to-column connections with or without stiffeners. To evaluate the contribution of the external endplate stiffeners to the mechanical behavior of the whole connection, tensile zone is represented by T-stub [4–6]. T-stub reinforced by backing-plates were also analyzed by Al-Khatab and Bouchair [7] using a finite element model to observe their global behavior as well as the evolution and the distribution of the contact pressure. The compression zone was analyzed in full beam-to-column connection as weak component in some studies [8–10] based on experimental investigations. An analytical approach [11], calibrated on the basis of existing experimental results, was proposed to analyze the stresses in the column web within beam-to-column connection. In the study, the possibility of isolating the web from the connection to determine its resistance is checked considering stiffened and unstiffened panels. A limited number of studies analyzed the behavior of unstiffened and stiffened web panels under compression for different cross-sections. Graham et al [12] performed an experimental investigation on American rolled beams with various types of stiffeners. They tested whole beam-to-column welded joints in bending and isolated beams under direct compression and

tension. They analyzed the relationship between the two types of tests illustrated in Fig. 1. They compared the experimental results with existing analytical design formula regarding the resistance making some adaptations for the cases with stiffeners. They indicated that the development of analytical approach for stiffeners needs the knowledge of their stress distribution and boundary conditions. The main analytical approach was based on the plastic resistance of compressed zone defined by the effective length. De Mita et al [13] realized an experimental study on usual European hot rolled profiles and compared the results with existing analytical formulas considering the resistance, the initial stiffness and the deformation capacity. The tests were based on double compressed web panels.

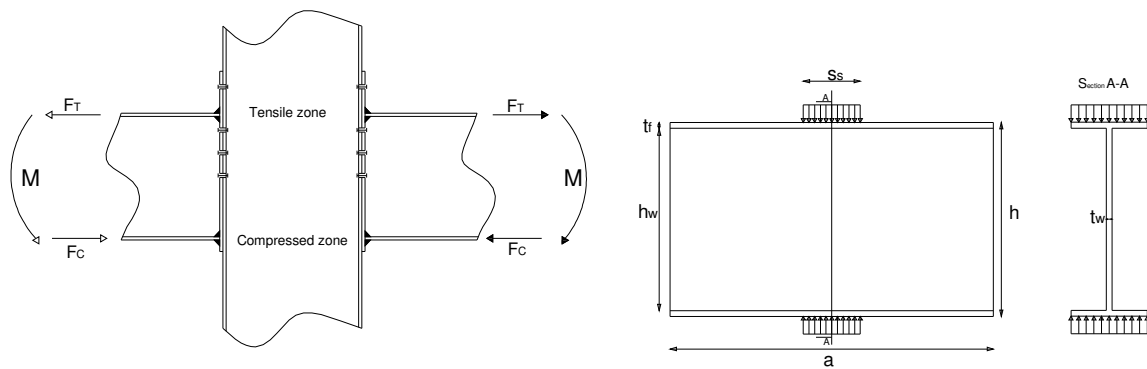


**Fig. 1.** Beam-to-column connection and model of compressed I beam panel.

The behavior of unstiffened panels subjected to patch loading has been widely studied through experimental, numerical and theoretical analysis. The failure modes of a panels under concentrated load have been considered as web folding. So, they are analyzed considering plastic hinges in the loaded flanges and web combined with the buckling capacity of the web. Thus, to obtain the maximum loads, researchers proposed several expressions of the elastic critical loads and physical models based on plastic analysis with potential plastic hinges and yield lines potentially occurring in the flanges and web panels [14,15]

Thereafter, the patch loading is covered by EN1993-1-5 [16] considering analogy with instability problems (named the  $\chi$ - $\lambda$  approach). With this approach, the plastic resistance is

reduced by a factor considering the instability. The prediction accuracy of this analytical approach has been evaluated using experimental and numerical results of steel plate girders locally loaded up to failure [17,18]. **The approach used in EN1993-1-5 [16] is given hereafter (Equation 1 to 4).**

$$F_u = \chi F_y \quad (1)$$

$$\chi(\bar{\lambda}) = \frac{0,5}{\bar{\lambda}} \leq 1 ; \bar{\lambda} = \sqrt{\frac{F_y}{F_{cr}}} \quad (2)$$

$$F_{cr} = 0.9k_F E \frac{t_w^3}{h_w} ; k_F = 3.5 + 2 \left( \frac{h_w}{a} \right)^2 \quad (3)$$

$$F_y = f_{yw} t_w \left( s_s + 2 t_f + 2t_f \sqrt{\frac{f_{yf}b_f}{f_{yw}t_w} + \frac{2k^2h_w^2}{t_f^2}} \right) \quad (4)$$

Recently, some studies proposed an adaptation of the formulas given by EN1993-1-5[16]. Mezghanni et al [19] followed the same procedures proposed by Lagerqvist [18] to determine the maximum strength of compressed sections using different boundary conditions. In all cases studied, the resistance of the compressed section is influenced by two failure modes which are the instability of the web panel that depends on its slenderness, and the local plastic mechanism.

To improve the resistance of web panels in compressed zones of connections, supplementary web plates or stiffeners can be used (EN1993-1-8 [1]). Various stiffener configurations are used in practice to reinforce the web panels. The most frequently used are the single sided, double sided and multi-leg flat stiffeners [20].

Stiffeners can be welded on one side of the plate (single sided), or on both sides (double sided). Usually bearing stiffeners are double sided, while intermediate web stiffeners are single sided. Depending on their positions, the stiffeners can be inclined, longitudinal or

transverse. Inclined stiffeners are used in the case of non-symmetric double-sided beam-to-column connections [3].

Longitudinal stiffeners are stiffeners in the direction parallel to that of the flanges. They are mainly used to reinforce the girders with large dimensions. Their behavior in compressed beams was studied using numerical analysis based on existing tests or theoretical models [21–24] Longitudinal stiffeners are also used to avoid web bend-buckling that may lead to a remarkable reduction of the flexural resistance of the girders [25,26]. Another important role of the longitudinal stiffeners is to control the lateral deflection of the girder webs.

Transverse stiffeners are installed in the direction perpendicular to that of the flanges [3,27]. The simple flat stiffener is the type usually used in modern constructions to resist compression and shear of the panels [28–30]. Transverse stiffeners, with a thickness at least equal to that of the stiffened panel, are welded on the full height of the web panel and the flanges. In bolted joints, the stiffener in the compression zone should be aligned with the beam flange (center of compression). Many numerical studies are carried out to determine the resistance of compressed plates or plate girders subjected to in plane compression. Choi et al [31] performed a finite element study to analyze the behavior of transverse stiffeners in web panels loaded in compression considering their stiffness requirements according to the AASHTO [27] specifications. Another numerical study was performed by Chacon et al [32] to define a mechanical formulation to estimate the strength of closely spaced transverse stiffeners in steel plate girders subjected to patch loading. K. Le Tran [33] explained the approach proposed by EN19933-1-5 to determine the resistance of transversally stiffened plates by one stiffener or more, subjected to uniform compression load. The calculation steps, based initially on longitudinal stiffeners, considers two types of behaviors and their interaction: column type buckling, plate type buckling and the interaction between plate and

column buckling through calibrated coefficient. The formulae used in EN1993-1-5 [16] are given in equations 5 to 17.

$$F_u = A_{c,eff} \frac{f_y}{\gamma_{M1}} \quad (5)$$

$$A_{c,eff} = \rho_c A_{eff,loc} + \sum b_{edg,eff} t \quad (6)$$

$$\rho_c = \chi_c + (\rho - \chi_c)(2 - \xi)\xi \quad (7)$$

$$\xi = \frac{\sigma_{cr,p}}{\sigma_{cr,c}} - 1 \quad (8)$$

column behavior

$$\sigma_{cr,c} = \frac{\pi^2 E I_{sl,1}}{A_{sl,1} a^2} \quad (9)$$

$$\chi_c = \frac{1}{\phi + \sqrt{\phi^2 - \bar{\lambda}_c^2}} \quad (10)$$

$$\phi = 0,5 [1 + \alpha_e (\bar{\lambda}_c - 0,2) \bar{\lambda}_c^2] \quad (11)$$

$$\alpha_e = \alpha + \frac{0,09}{e} \quad (12)$$

$$\bar{\lambda}_c = \sqrt{\frac{\beta_{A,c} f_y}{\sigma_{cr,c}}} \quad (13)$$

Plate behavior

$$\sigma_{cr,p} = k_{\sigma,p} \sigma_E \quad (14)$$

$$\rho = \frac{1}{\bar{\lambda}_p} - \frac{0,22}{\bar{\lambda}_p^2} \quad (15)$$

$$\bar{\lambda}_p = \sqrt{\frac{\beta_{A,c} f_y}{\sigma_{cr,p}}} \quad (16)$$

$$\beta_{A,c} = \frac{A_{sl,1,eff}}{A_{sl,1}} \quad (17)$$

The present paper proposes an experimental, numerical, and analytical study of transverse stiffeners welded to the web panel subjected to opposite compression loading. Indeed, this type of stiffeners can be one of the most appropriate choices to reinforce the compressed zone in the column of beam-to-column connections. Different lengths and positions of the stiffeners on the height of the web panels are tested. The tested specimens can represent the

behavior of the compression zone in fully or partially stiffened panels. Twelve hot-rolled and welded I-sections with stiffeners were tested until failure. Tests are used to observe the behavior of stiffened web panels in compression and to validate a finite element model built using the CAST3M software [34]. The comparison between the experimental and numerical results is based on the maximum strengths, the load-displacement curves and the observed failure modes.

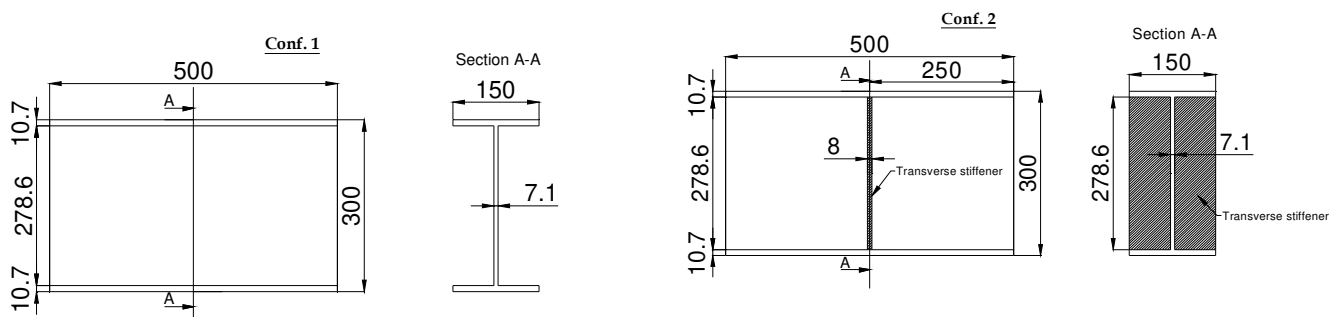
## 2. Experimental tests

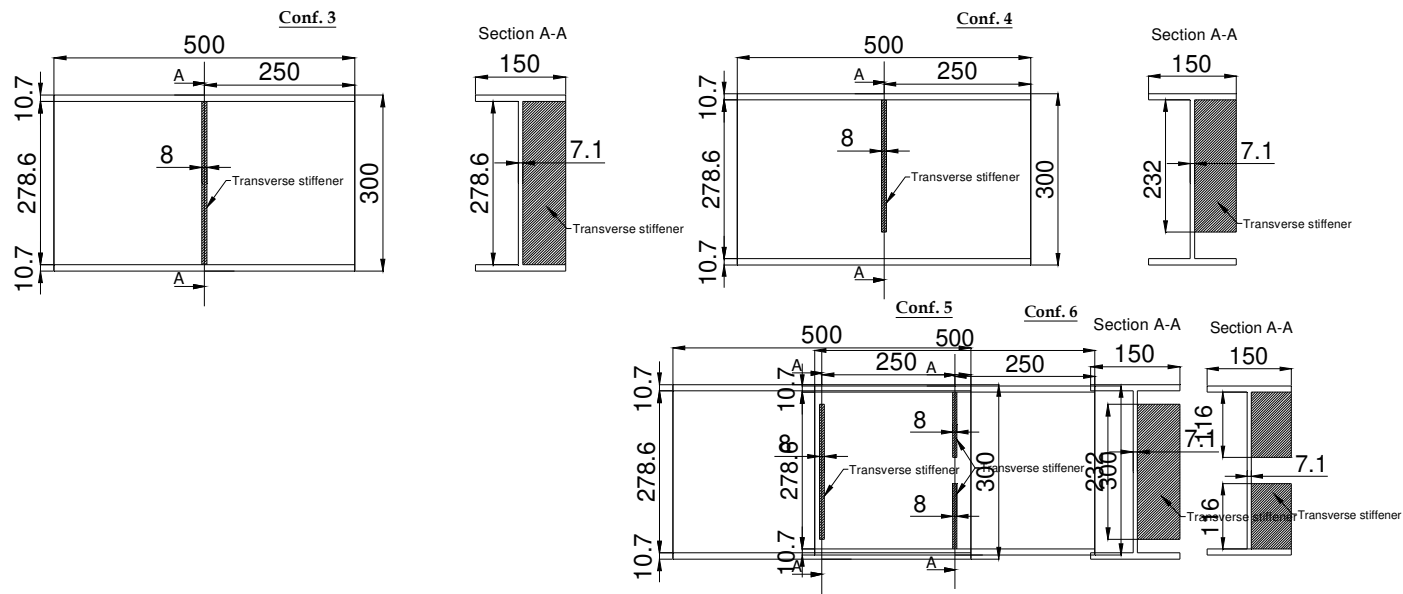
### 1.1. Test specimens

The twelve tested specimens aim to represent the compressed zone in a column web panel of double-sided beam-to-column connection. Six specimens were taken from hot rolled I sections and the other six are welded I sections. In each group of six specimens, one is without stiffener to obtain a reference as unreinforced panel. The five stiffened specimens have different positions or dimensions of stiffeners (see Fig.2 and Table 1). The web thicknesses are equal to 5.5, 7.1 or 12.3 mm. The stiffeners thicknesses are equal to 5.5 and 8 mm. The stiffeners are either welded on the full height of the web and the flanges or on a part of the web and flanges or on a part of the web height (see Fig.2).

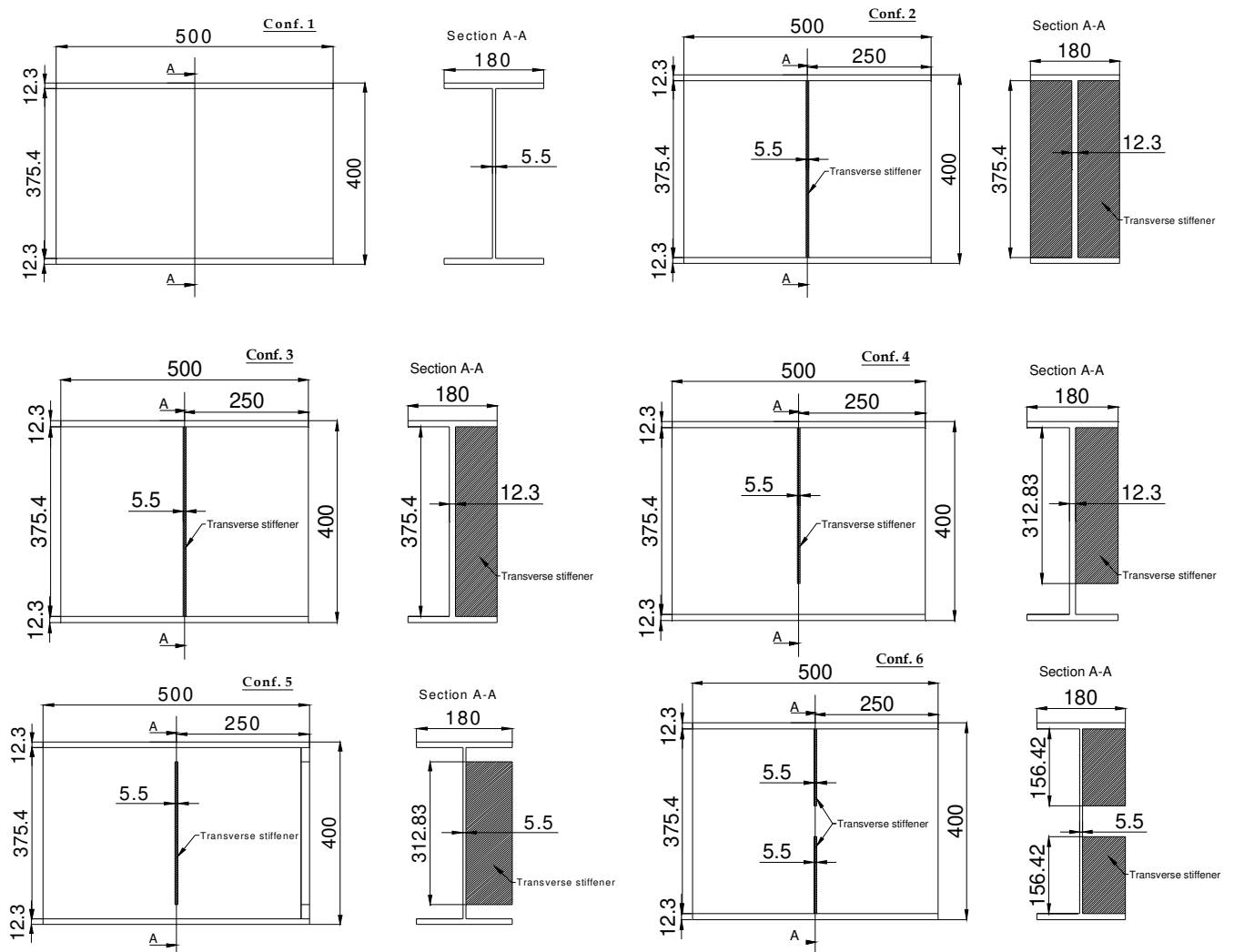
The stiffeners depths are chosen with reference to the web panel height leading to:

- $h_s = h_w$  (for stiffeners welded on the full height of the web panel and the flanges),
  - $h_s = \frac{5}{6} h_w$  (for stiffeners welded on a part of the web panel height and/or not on the flanges),
- see Fig.2.





(a) Specimens from hot rolled I-sections



(b) *Specimens from welded I-sections*

**Fig. 2.** Configurations of the tested specimens with transverse web stiffeners

**Table 1**

Description of the tested specimens according to the stiffeners positions

<b>Model</b>	<b>Description</b>
<b>Conf. 1</b>	Unstiffened section, “1.U”
<b>Conf. 2</b>	Double transverse stiffeners on the <b>Full</b> web height (welded to web and flanges), “2.FD”
<b>Conf. 3</b>	Single transverse stiffener on the <b>Full</b> web height (welded to web and flange), “3.FS”
<b>Conf. 4</b>	<b>Partial</b> transverse stiffener (welded to web and <b>one</b> End flange), “4.P1E”
<b>Conf. 5</b>	<b>Partial</b> transverse stiffener on the <b>Central</b> part of the web height (welded to web), “5.PC”
<b>Conf. 6</b>	<b>Partial</b> transverse stiffener on two parts of the web (welded to web and <b>two</b> End flanges), “6.P2E”

The main names and descriptions of specimens according to the stiffeners positions are given in Table 1. In addition, each specimen is named using H, for hot rolled sections, or  $W_{\lambda_1 \text{ or } \lambda_2}$ , for welded sections.  $W_{\lambda_1}$  and  $W_{\lambda_2}$  correspond respectively to the web thickness of 5.5 mm and 12.3 mm, respectively.  $\lambda$  is the slenderness calculated as  $\frac{h_w}{t_w}$ .

### 1.2. Mechanical properties

Mechanical properties of materials are determined through tensile tests on coupons [35] cut from web plates, flanges and stiffeners. Results of tensile tests for both yield and ultimate stresses are summarized in Table 2.

**Table 2**

Mechanical properties of steel used in the tested specimens

<b>coupon</b>	<b>thickness (mm)</b>	<b><math>f_y</math> (MPa)</b>	<b><math>f_u</math> (MPa)</b>
<b>Flange</b>	10.7	269.3	408.4
<b>Web</b>	7.1	304.4	421.7
<b>Stiffener</b>	8	320	448
<b>Web / stiffener</b>	5.5	360	424
<b>Web / flange</b>	12.3	358.4	504

*1.3. Instrumentation and test setup*

The tests were carried out using a compression testing machine (see Fig.3). The compressive force is applied through two symmetrical rigid steel plates on both sides with a length  $S_s$  of 100 mm (see Fig. 3) applied on the whole width of the flanges. The load is applied with a constant displacement rate and the test stopped when the maximum load is reached followed by significant displacement developed in the post-failure stage. The load decrease beyond the maximum value represents the instability of the specimen. The tested specimens are shown in Fig.4. The measured displacement is that of the mobile part of the testing machine. This mobile part introduces the load through a hinged rigid plate with small free rotation.

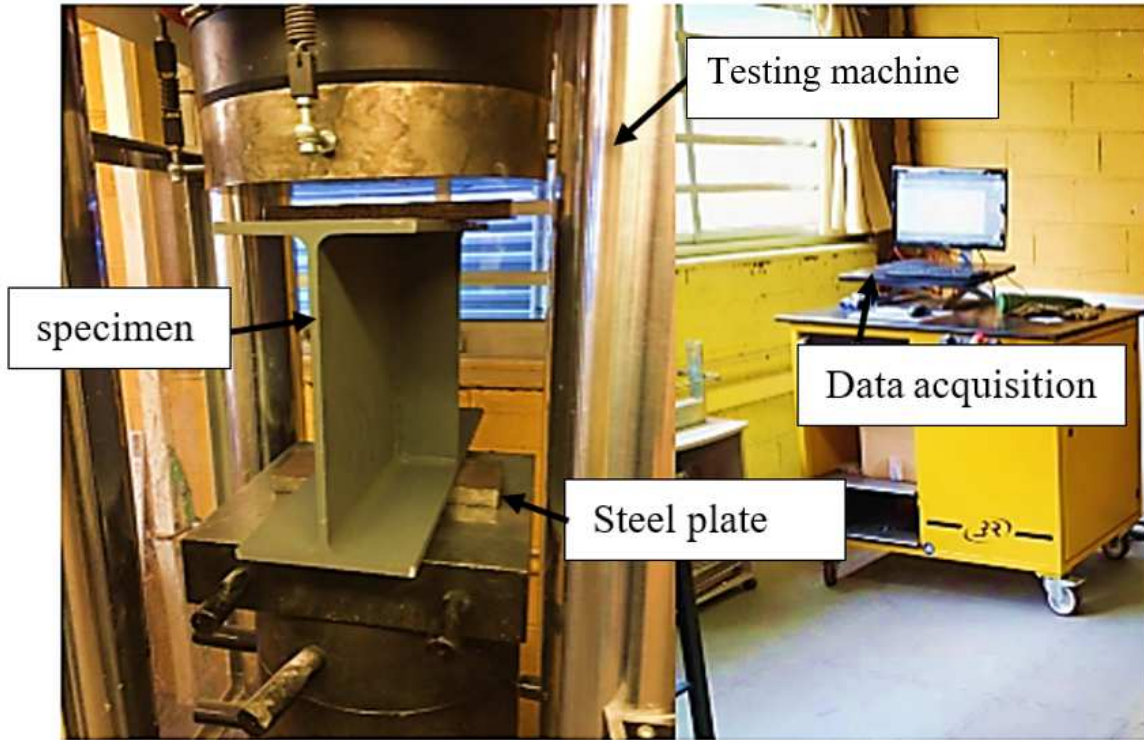


**Fig. 3.** Experimental tests setup

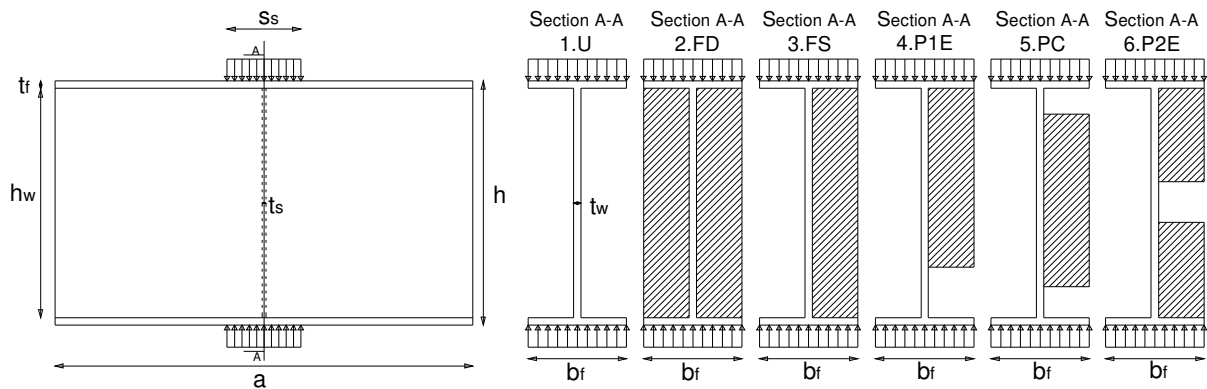
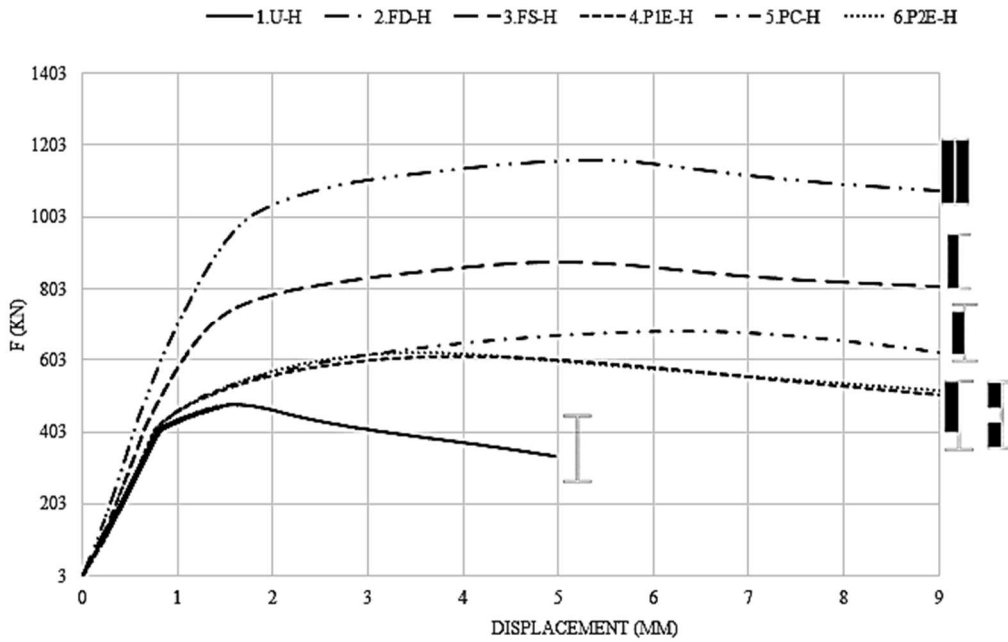


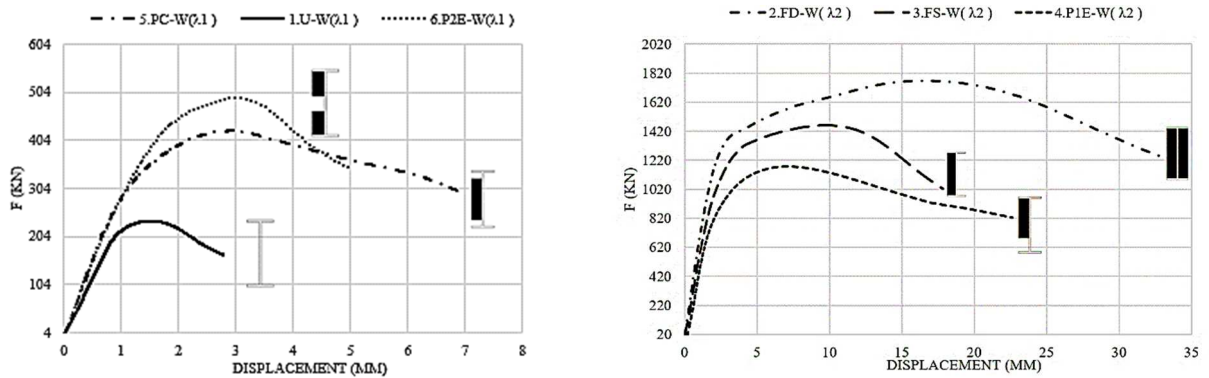
**Fig. 4.** Loading system and tested specimens with and without stiffeners

The comparison of experimental load-displacement curves between specimens having the same geometries with different sets of stiffeners (full, partial) is made to show the contribution of the stiffeners. As shown in Fig.5 (a) for hot rolled I-sections, differences appear from the linear phase. As the tests are realized in the same conditions, this confirms the fact that initial rigidities of panels are different with higher values for the cases with

stiffeners. The highest stiffness is obtained for the full-length double-sided stiffeners. In non-linear phase, all cases except the unstiffened one, show a long plastic phase before the load decrease representing the instability. Fig.5 (b) combines the experimental curves for welded I-sections considering each of the two web thicknesses. The full height stiffeners show a plastic phase longer than that of unstiffened and partially stiffened web panels.



(a) hot rolled I-sections



(b) welded I-sections

**Fig. 5.** Experimental results

### 3. Numerical model

### 3.1. Finite element model development

Finite element models were constructed using CAST3M software with three nodes shell elements (DKT elements). Finite element mesh was chosen based on a mesh convergence study (see Fig.6).

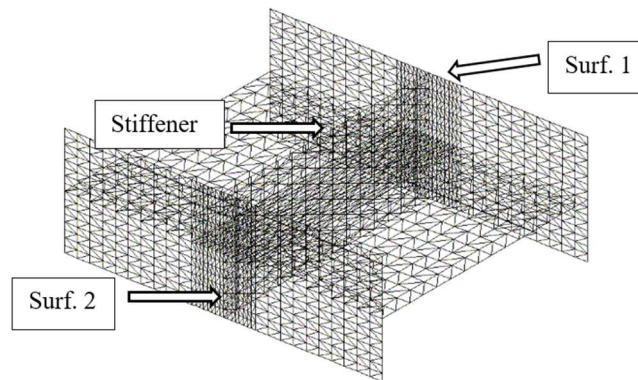


**Fig. 6.** Meshing of the specimen with stiffener.

Boundary conditions are chosen in order to represent the tests, they were applied on both loading surfaces Surf. 1 and Surf. 2 (see Fig.7).

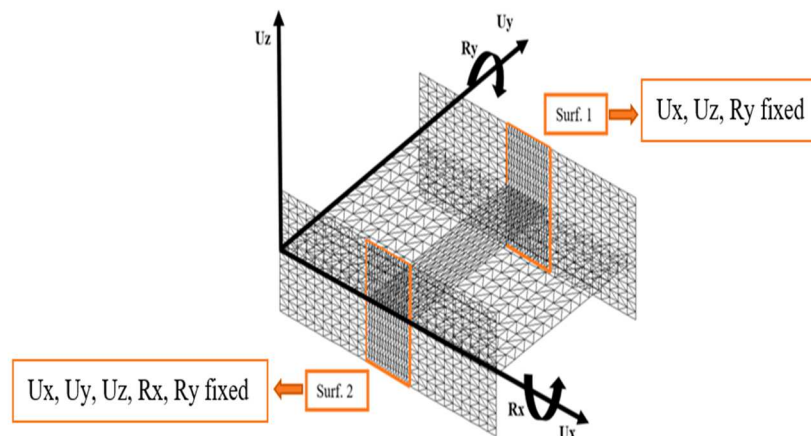


**Fig. 7.** Boundary conditions

The mechanical characteristics of steel are based on the yield limits obtained by coupon tests taken from different parts of the specimens (see Table 2). Elastic perfectly plastic model is

chosen to represent the material behavior. In fact, two stress-strain curves were used: elastic perfectly plastic and elastic-plastic with strain-hardening representing the real curve obtained from tensile tests (Fig. 8).

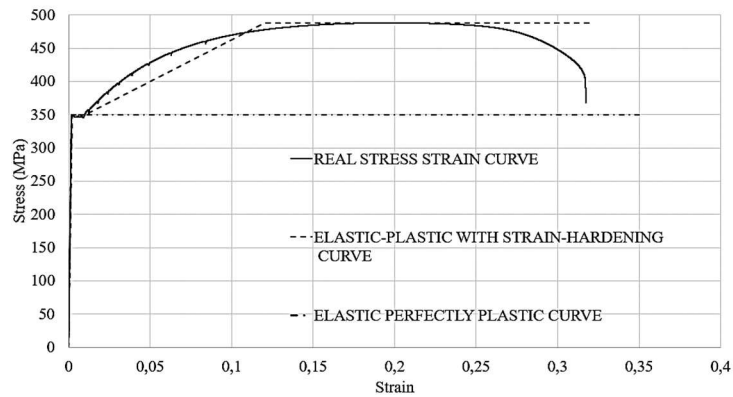
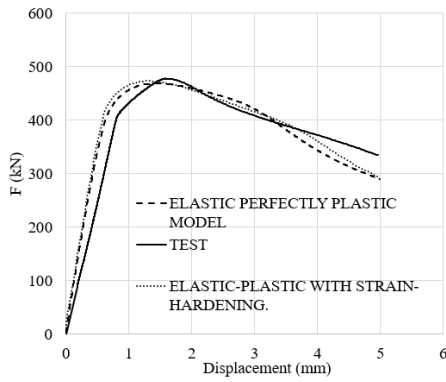


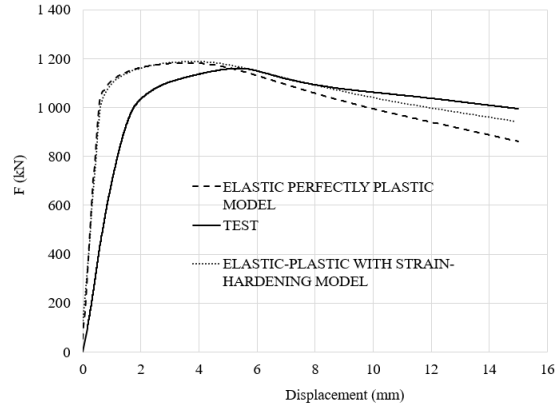
**Figure 8:** Stress strain curves (real and models)

The comparison shows that the elastic perfectly plastic model represents well the mechanical behavior of the unstiffened and stiffened panels. Examples of the comparisons for two configurations (1.U-H and 2.FD-H) are shown in Fig. 9. This small difference can be explained by the fact that a plastic plateau exists for the two stress-strain curves in addition to the failure reached mainly in bending with limited plastic deformation.

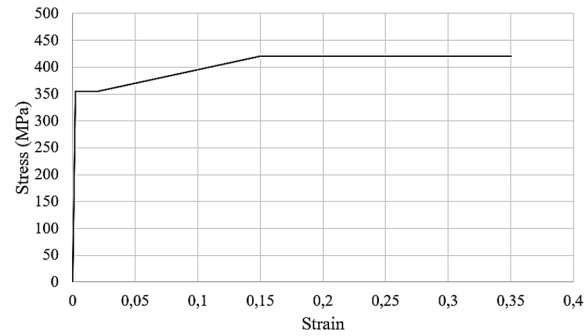
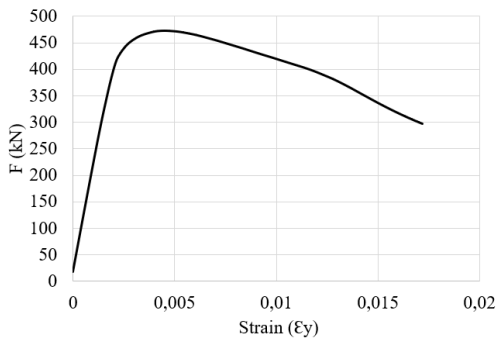
A representation of the load-strain curve of the 1.U-H configuration is presented in Fig.10. It can be observed that the deformation corresponding to the maximum load belongs to the first plastic plateau of the stress-strain curve with strain-hardening. That explain the fact that elastic perfectly plastic model represents well the behavior of most of the tests.



(a) unstiffened panel (1.U-H)



(b) double stiffened panel (2.FD-H)

**Fig.9. Load-displacement curves: comparison of two material laws****Fig.10. Load-strain and stress-strain curves**

Nonlinear behavior of materials is combined with large displacements to represent the real behavior of the specimens. Thus, incremental calculation with displacement control is performed to control the descending part of the load-displacement curves. Each calculation is performed on two steps. The first one concerns an Eulerian calculation used to define the buckling mode of the specimen with or without stiffeners. Then, the initial geometrical imperfection is defined using the first buckling mode obtained. The second step is the non-linear analysis, elastic-plastic with large displacements, performed on the deformed shape of the specimen to obtain the load-displacement curve including the post-critical part of the curve.

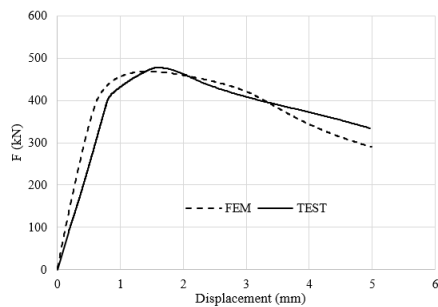
The amplitude of imperfection is taken equal to  $h_w/200$ . This choice is based on the EN1993-1-5 [16] annex-C that defines the imperfection amplitude for compressed webs as  $\min(a/200; h_w/200)$ .

### 3.2. Finite element model validation

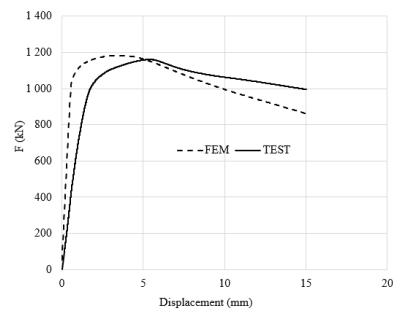
The comparison between the experimental and numerical results concern the maximum loads, the load-displacement curves and the failure modes. This comparative study aims at validating the numerical model.

#### 3.2.1. Load-displacement curves (FE and Exp)

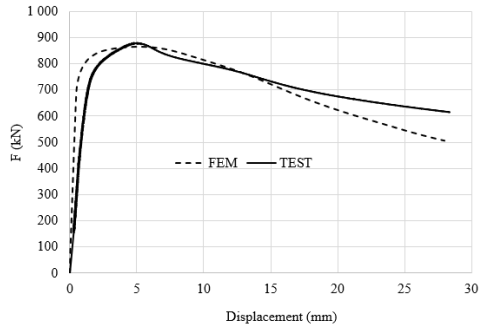
Load-displacement curves are presented in Figure 11. The displacement is taken from a point under the applied load. The comparisons between the experimental curves and those from FEM show that the finite element model represents well the global behavior of the specimens including the post-failure part. Nevertheless, it exists some deviations mainly for the displacements where the experimental tests include the imperfect contact between the testing machine and the specimen flange. **The real boundary conditions and the possible influence of the contact between the loaded flanges and the testing machines plates are not considered by the numerical model.**



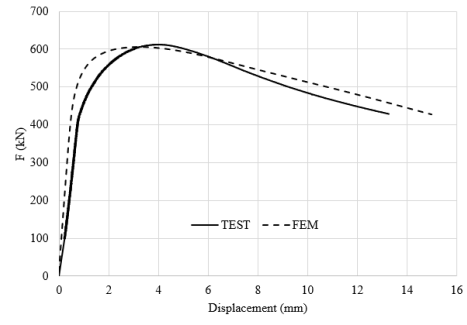
Load-displacement curves of 1.U-H



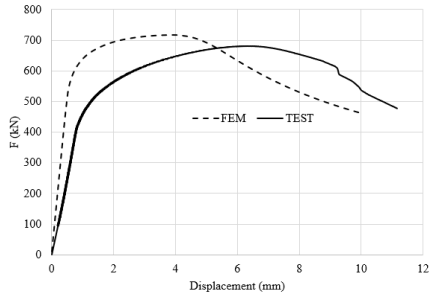
Load-displacement curves of 2.FD-H



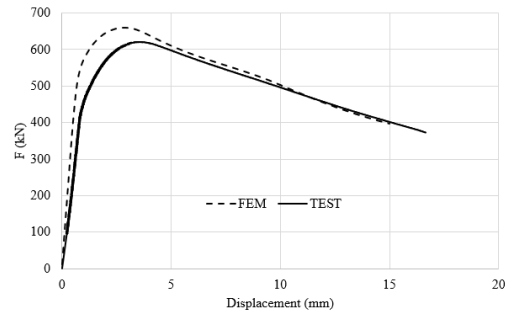
Load-displacement curves of 3.FS-H



Load-displacement curves of 4.P1E-H

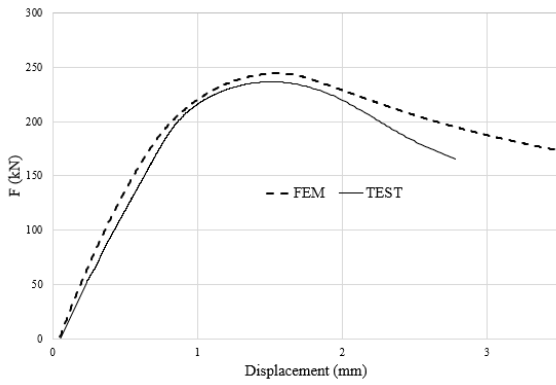


Load-displacement curves of 5.PC-H

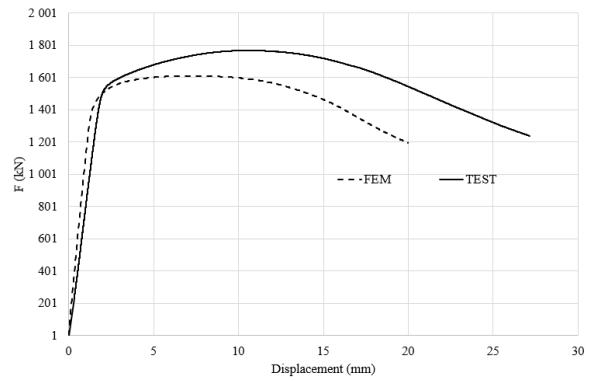


Load-displacement curves of 6.P2E-H

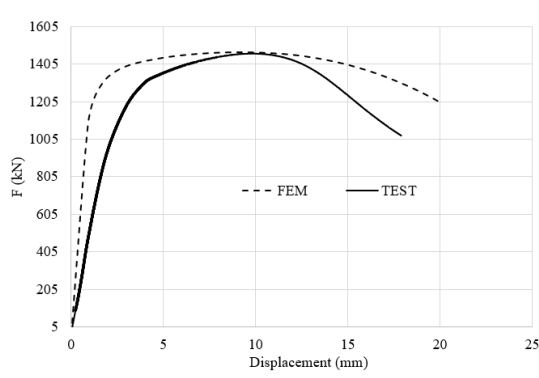
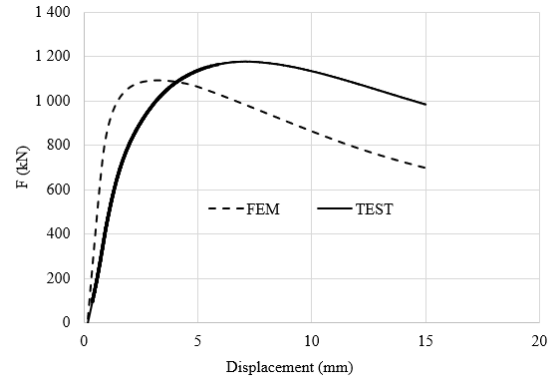
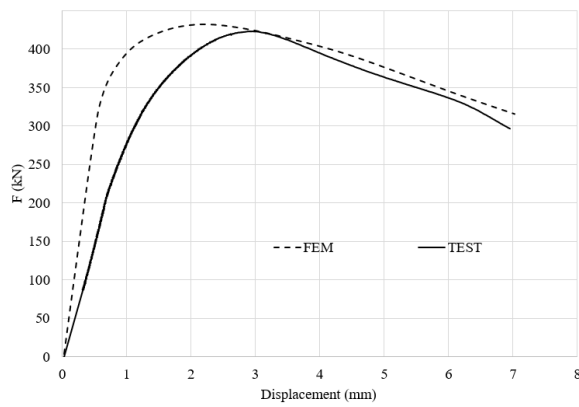
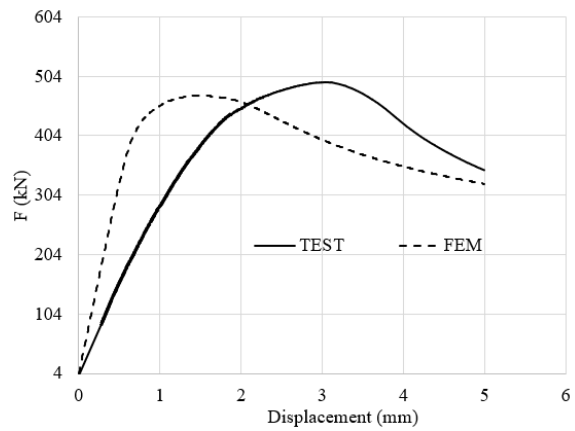
(a) Hot rolled I-sections



Load-displacement curves of 1.U-W <sub>$\lambda_1$</sub>



Load-displacement curves of 2.FD-W <sub>$\lambda_2$</sub>

Load-displacement curves of 3.FS- $W_{\lambda_2}$ Load-displacement curves of 4.P1E- $W_{\lambda_2}$ Load-displacement curves of 5.PC- $W_{\lambda_1}$ Load-displacement curves of 6.P2E- $W_{\lambda_1}$ (b) *Welded I-section***Fig. 11.** Comparison of load-displacement curves (FEM and tests)

Regarding the stiffness, a difference is observed between FEM and test curves. This difference can be explained mainly by the displacement measurement which is based on the mobile part of the testing machine. Another explanation can be related to the initial imperfection. Indeed, it can be observed that most important differences correspond to the cases of welded profiles. Those profiles usually have more imperfections in parallelism which may induce eccentric load and more out of plan bending of the web. This geometrical default is illustrated in Fig.12.

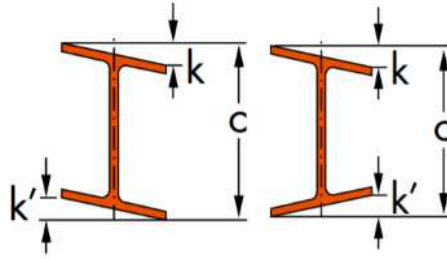


Figure 12 : Illustration of out of square tolerance

In the case of cross laminated sections, the accepted value of out of square is defined as  $k+k' < 1.5\text{mm}$ . This imperfection may have an impact on transverse load mechanical behavior as the applied load has some eccentricity with the web. The comparative study presented hereafter aims at studying the influence of the point load eccentricity on the mechanical behavior of panels submitted to transverse compression.

This numerical study concerns the configurations corresponding to configurations 1.U- $W_{\lambda_1}$  (PRS400 without stiffener) and 4.P1E- $W_{\lambda_1}$  (PRS 400 with partial stiffener connected to the flange). The numerical models are constructed considering 3 eccentric load positions. Indeed, during the experimental tests, even if the load is initially applied at the end of the flange, as the flange rotates, the loaded zone migrates to the web until the loaded flange becomes horizontal. Thus, the observed behavior for the 3 modeled situations do not aim at representing the test, but to evaluate the influence of various load eccentricities on the panel stiffness and strength. Figure 13 presents the 3 load positions that have been evaluated using FEM. The vertical displacement considered is that of the loaded zone as it corresponds to the experimental measured displacement.

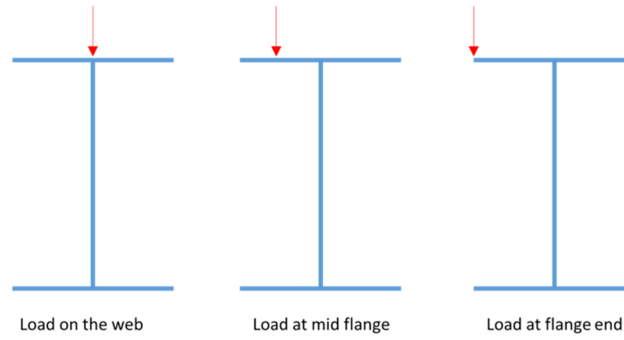


Figure 13. Three positions of load analyzed to evaluate the boundary conditions of tests

The values of initial stiffness for the three situations of loading are given in Table 3. The difference observed between test and FEM can be explained mainly by the boundary conditions of the contact between the testing machine and the imperfect specimen. The influence of the initial imperfection of the web is observed on two examples with two imperfections ( $h_w/90$  and  $h_w/200$ ) (see Fig. 14). Its effect on the initial stiffness is less than that of the loading conditions (Table 3).

Table 3: Evolution of the initial stiffness depending on the load introduction

Specimen	Load at the web	Load at mid flange	Load at flange end
1.U- $W_{\lambda_1}$	146.5	5.1	1.6
4P1E- $W_{\lambda_1}$	233.7	44.1	24.1

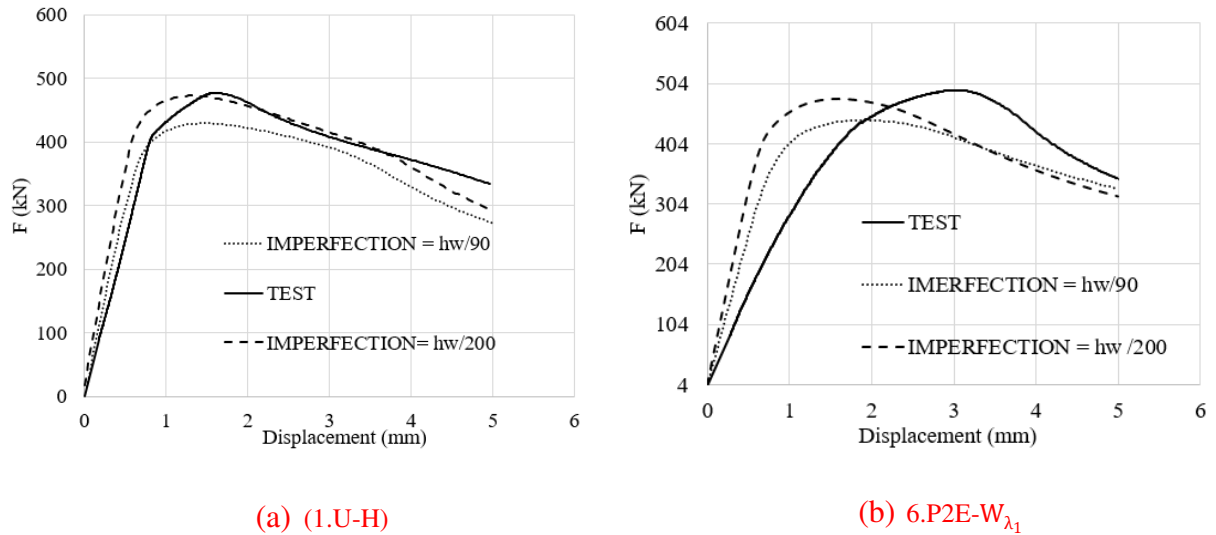


Figure 14: Comparison of test result with FEM results in case of  $h_w/90$  and  $h_w/200$  imperfections

### 3.2.2. Maximum strengths

The maximum loads of tested specimens obtained from tests ( $F_{u,Test}$ ) and finite element model ( $F_{u,FEM}$ ) are summarized in Table 5. The comparison between the experimental and numerical values of resistance shows that the finite element model predicts accurately the experimental results (maximum difference of  $\pm 7\%$  in all cases).

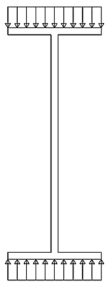
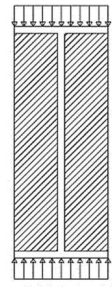
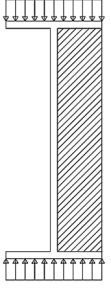
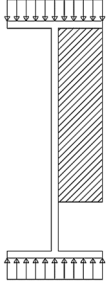
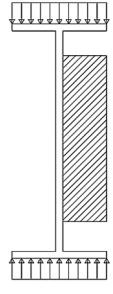
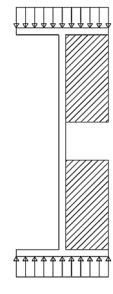
In hot rolled I-sections, all specimens described in table 4 have the same cross-section dimensions, the only varying parameter is the stiffener configuration, either partial or full-length stiffener. As expected, the resistance of fully stiffened panels is higher than that of partially stiffened or without stiffeners. It can be observed that compared to the specimen without stiffener, the maximum load increases by 83% for one sided full-length stiffener and by 143% for double-sided full-length stiffener. The partial length stiffeners increase the resistance by 30% to 42%. Thus, the partial length stiffeners can increase the load carrying capacity of the profile. Furthermore, for a given partial stiffener length, it can be observed that the position of the partial stiffener influences the load carrying capacity (see specimens 4.P1E-H, 5.PC-H and 6.P2E-H in table 4). The configuration 5.PC-H (stiffener located at the web mid-height) shows higher resistance than the stiffener with the same length but welded at

the bottom or the top of the web (configurations 4P1E-H and 6P2E-H). Indeed, both configurations 4P1E and 6P2E have a longer continuous unstiffened web part (see table 4).

In the case of welded I-sections, all the web panels have the same height but two different thicknesses. The specimens 1.U- $W_{\lambda_1}$ , 5.PC- $W_{\lambda_1}$  and 6.P2E- $W_{\lambda_1}$  are with a web thickness of 5.5 mm. The specimens 2.FD- $W_{\lambda_2}$ , 3.FS- $W_{\lambda_2}$  and 4.P1E- $W_{\lambda_2}$  are with a web thickness of 12.3mm. For all cases, the stiffener has a thickness of 5.5mm. As observed, in table 4, for the hot rolled sections, the resistance of fully double-stiffened panel (2.FD- $W_{\lambda_2}$ ) is higher than that of fully single stiffened (3.FS- $W_{\lambda_2}$ ) or partly stiffened one (4.P1E- $W_{\lambda_2}$ ). Comparing the different partial stiffener configurations (5.PC- $W_{\lambda_1}$ , 6.P2E- $W_{\lambda_1}$ ) it can be observed that the configuration with stiffeners welded at the top and bottom of the profile (6P2E) exhibit the highest compressive strength.

**Table 4**

Maximum strengths for the tested configurations (in kN)

												
	1.U- H	1.U- $W_{\lambda_1}$	2.FD- H	2.FD- $W_{\lambda_2}$	3.FS- H	3.FS- $W_{\lambda_2}$	4.P1E- H	4.P1E- $W_{\lambda_2}$	5.PC- H	5.PC- $W_{\lambda_1}$	6.P2E- H	6.P2E- $W_{\lambda_1}$
$F_{u,Test}$	478	236.9	1160.9	1768	876.8	1461	612.3	1177.8	681.9	423.9	622	493.3

From Table 4, it can be observed that the effect of the stiffener increases with the increase of the web panel slenderness. A double-sided stiffener brings between 17 and 24% of the resistance compared with the single-sided stiffened panel in these two cases of study (hot rolled and welded I sections). It can be observed that in the case of hot rolled profile, both

configurations 4 and 6 give a similar maximum load, and configuration 5 exhibits an maximum load slightly greater. This result can be considered logical regarding that the web length between the stiffener and the flanges is divided by 2 in configuration 5 compared to configurations 4 and 6. Table 5 compares the finite elements results with experimental results and it can be seen that the tendencies remain the same. Indeed, even without considering the fillet corner for the hot profile, the same observations can be done with similar maximum load values.

The difference of results given in table 5 is calculated using the equation below;

$$\text{Difference (\%)} = \frac{F_u^{\text{test}} - F_u^{\text{FEM}}}{F_u^{\text{FEM}}} \times 100$$

**Table 5**

Comparison of resistances obtained from tests and finite element model.

<b>Hot rolled I-sections</b>			
<b>Specimen</b>	$F_{u,\text{Test}}$ (kN)	$F_{u,\text{FEM}}$ (kN)	Difference (%)
<b>1.U-H</b>	478	468.6	2.0
<b>2.FD-H</b>	1160.9	1183.3	-1.9
<b>3.FS-H</b>	876.8	865.9	1.3
<b>4.P1E-H</b>	612.3	606.8	0.9
<b>5.PC-H</b>	681.9	718.9	-5.1
<b>6.P2E-H</b>	622	661.1	-5.9
<b>welded I-sections</b>			
<b>Specimen</b>	$F_{u,\text{Test}}$ (kN)	$F_{u,\text{FEM}}$ (kN)	Difference (%)
<b>1.U-W<math>\lambda_1</math></b>	236.9	244.5	-3.1

<b>2.FD-W<sub><math>\lambda_2</math></sub></b>	1768	1807.7	-2.2
<b>3.FS-W<sub><math>\lambda_2</math></sub></b>	1461	1482.1	-1.4
<b>4.P1E-W<sub><math>\lambda_2</math></sub></b>	1177.8	1091.5	7.9
<b>5.PC-W<sub><math>\lambda_1</math></sub></b>	423.9	427.6	-0.9
<b>6.P2E-W<sub><math>\lambda_1</math></sub></b>	493.3	471.8	4.6

Consequently, it can be seen that for two different profiles which exhibit two different web slenderness, the best partial stiffening solution differs. The use of partial stiffener can be compared to one side full stiffener. For both profiles, the length of the stiffener has been reduced of 17% compared to the full web stiffener. It is then proposed to look at the reduction of strength induced by this reduction of stiffener length.

In the case of hot rolled profile, configuration 5 has the higher strength with a reduction of strength compared to full web stiffener of 22%, whereas the other two partial stiffeners reduce the strength of 30% approximately. Concerning welded panel, it can be seen that configuration 4 gives the best results, with a reduction of strength of 20% with the full web stiffener, whereas both configurations 5 and 6 lead to a reduction of 70 and 66% of the strength. These observations can be done also with the finite element results.

When comparing the maximum strengths of partly stiffened panels (see Fig.15 and 16), it was observed that when slenderness of the panels is  $\lambda = 39.24$  the configuration 5.PC-H is more resistant than configuration 6.P2E-H. However, when the slenderness of the panels is  $\lambda = 68.25$ , the configuration 6.P2E-W <sub>$\lambda_1$</sub>  is more resistant than configuration 5.PC-W <sub>$\lambda_1$</sub>  (see main configurations in Fig. 17).

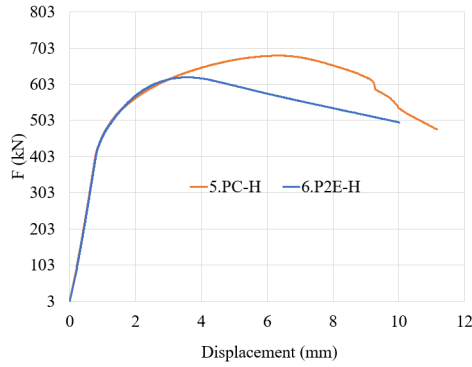


Figure 15: Experimental load-displacement curves (5.PC-H and 6.P2E-H)

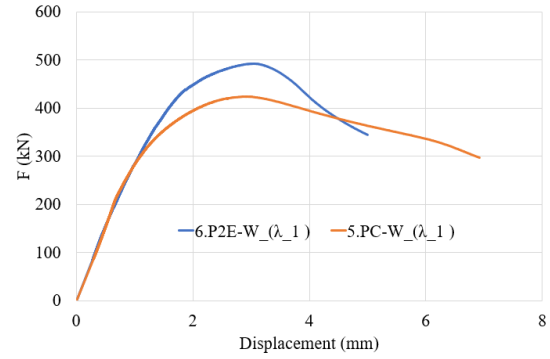


Figure 16: Experimental load-displacement curves (5.PC- $W_{\lambda_1}$  and 6.P2E- $W_{\lambda_1}$ )

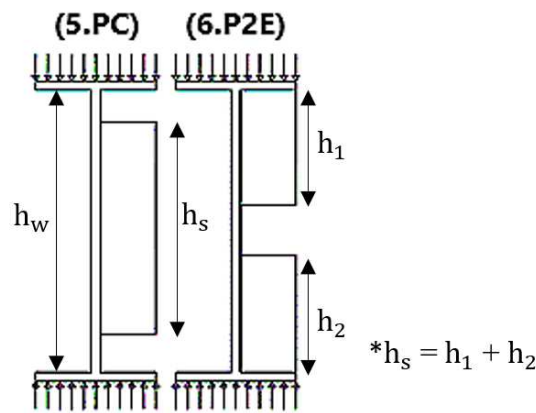


Figure 17: Configurations for parametric study

To explain the behavior of local stiffened panels of the two configurations listed in figure 17, the finite element model has been used in a parametric study evaluating the influence of the web panel slenderness ( $\lambda = \frac{h_w}{t_w}$ ) varying from  $\lambda = 30$  to  $\lambda = 70$

The two limits of the parametric study are taken to cover the two slenderness of the panels used in the experimental tests.

The study used stiffeners with two height ratios  $h_s = 5h_w/6$  (dimension taken in the experimental tests) and  $h_s = 3h_w/6$ . The results are summarized in Table 6, where the differences are calculated as:

$$\frac{F_u(5.PC) - F_u(6.P2E)}{F_u(6.P2E)} \times 100.$$

**Table 6**

Comparison between the resistance of panels in 5.PC and 6.P2E in function of the slenderness

<b>hs = 5hw/6</b>	<b><math>\lambda = h_w/5,5</math></b>	<b><math>F_u</math> (5.PC)</b>	<b><math>F_u</math> (6.P2E)</b>	<b>Difference %</b>
	30	468.2	431.1	8.6
	40	432.3	403.8	7.1
	50	401.7	417.2	-3.7
	60	335.6	426.5	-21.3
	70	308.7	430.6	-28.3
<b>hs = 3hw/6</b>	<b><math>\lambda</math></b>	<b><math>F_u</math> (5.PC)</b>	<b><math>F_u</math> (6.P2E)</b>	<b>Difference %</b>
	30	365.6	423.5	-13.7
	40	324.9	375	-13.4
	50	296.7	342.1	-13.3
	60	267	317.4	-15.9
	70	230.4	291.5	-21.0

In the case of a stiffener height equal to  $5h_w/6$ , it appears that if the slenderness of the web panel is under 50, stiffener attached to the two flanges offers less resistance than the central stiffener. However, if the length of the stiffener is ( $hs = 3h_w/6$ ), it appears that the stiffener welded to the flanges gives the optimal resistance in comparison with a central partial stiffener for all studied values of web panel slenderness.

The length of the stiffener is an important parameter that affects the behavior of the panels with transverse stiffeners. It informs about the optimal configuration in the case of local stiffened panels.

### 3.2.3. Failure modes (FE and Tests)

The failure modes of the tested hot rolled I-sections and welded I-sections are summarized in Fig.18. The photos were taken after each experimental test. The failure modes show the localized deformations associated to the specimens. For the panel in Fig.18 (a), the web is the only element that is deformed. It undergoes a buckling in the form of a half-wave. Regarding the panels in Fig.18 (b) and Fig.18 (c), the web deforms in an asymmetrical manner on both sides of the stiffener and the stiffener is buckled. This shows a torsional flexional buckling where the stiffener is buckled with an angle of rotation around the flexural axis. The web of the panel in Fig.18 (d) undergoes a deformation near the underside of the stiffener which does not deform with a pronounced rotation of the unstiffened part of the web. Thus, the stiffener reinforces the stiffened part in bending and plays the role of a load transmitter to the unstiffened part of the web panel. Regarding the web panel in Fig.18 (e), the web is deformed on its unstiffened parts at the ends of the stiffeners. It undergoes a half-wave bending while the stiffener does not deform, the flanges undergo a deformation in the direction of the load application, that can be similar to the first theorem of limit analysis that define potential plastic hinges in the flanges and potential yield lines within the web panel from either side of the intermediate stiffener. Finally, it is observed that for the panel in Fig.18 (f), the unstiffened web part is the only element which is deformed in bending and the stiffener remains undeformed. This case can be considered similar to that in Fig.18 (d).

For welded I-section, in the unstiffened panel (Fig.18 (g)), the web is the only element that deformed, its thickness is the lowest and the flanges are undeformed.

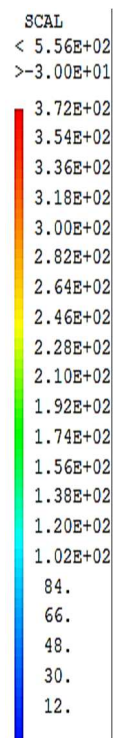
It should be noticed that for the configurations shown in Fig.18 (k) and Fig.18 (l), where the stiffener and the web have the same thickness, the stiffened web is deformed but with a less important amplitude than the unstiffened one. It was also noticed that for the specimen of Fig.18 (k), the flanges are plastified around the loading points. That can be the source of

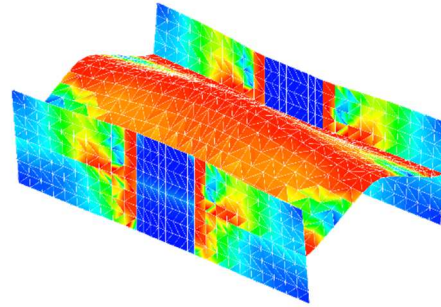
decrease of the maximum load value. In the case of fully stiffened panels by double or simple stiffener (Fig.18 (h) and Fig.18 (i)), the stiffener is the most affected section, and it undergoes buckling with different shapes.

However, in Fig.18 (j), the deformation is localized in the unstiffened part of the web. The stiffener, although thinner than the web, plays the role of load transmitter to the unstiffened part of the web. The flanges remain undeformed. However, they were locally yielded in the cases with symmetrical full height stiffeners (see Fig.18 (h) and Fig.18 (i)).

The deformed shapes of the unstiffened panels shown in Fig.18 (a) and Fig.18 (g) have some similarities with those observed in partially stiffened specimens shown in Fig.18 (e), Fig.18 (f), Fig.18 (k) and Fig.18 (l). Observing the specimens with fully stiffened web in hot-rolled I sections (Fig.18 (b), Fig.18 (c)) and welded I-section (Fig.18 (h), Fig.18 (i)), the deformed shape of the stiffener (two waves or one local wave) depends on its thickness compared to that of the web. If the stiffener has the same thickness as the web, it undergoes one full wave. Although having a stiffener thickness lower than that of the web, the partly stiffened panel in Fig.18 (j) behaves in a similar way as the panel with the same stiffener but a thickness equal to that of the web.

Typical deformed shapes corresponding to the experimental failure modes are predicted by the numerical models. Fig.18 shows some cases where the pictures taken after tests are compared to the deformed shapes obtained at the final step of the finite element model. Thus, the numerical model can be considered as sufficiently accurate to represent the behavior of web panels with or without transverse stiffeners loaded in compression.

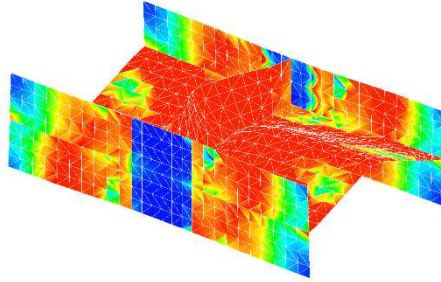
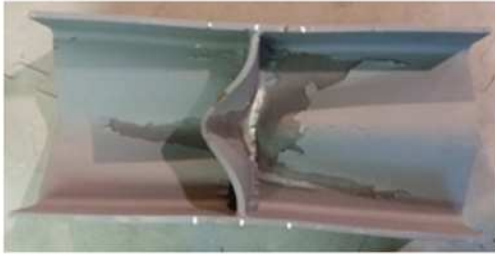




---

(a) Failure mode of 1.U-H

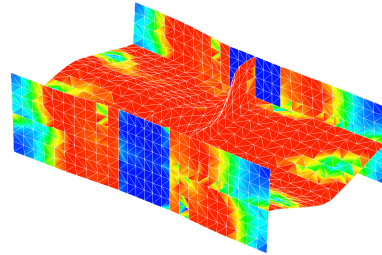
---



---

(b) Failure mode of 2.FD-H

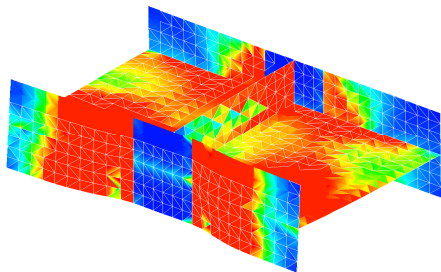
---



---

(c) Failure mode of 3.FS-H

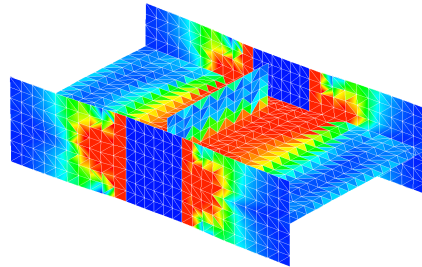
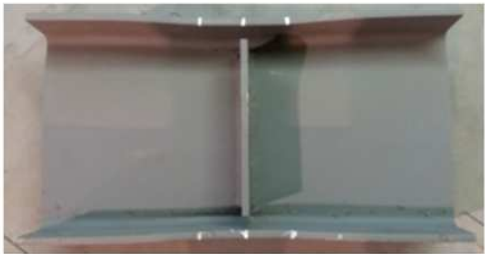
---



---

(d) Failure mode of 4.P1E-H

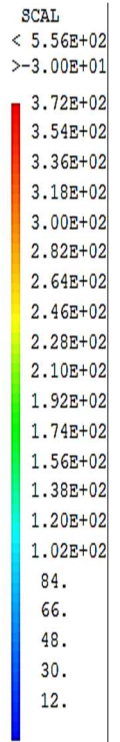
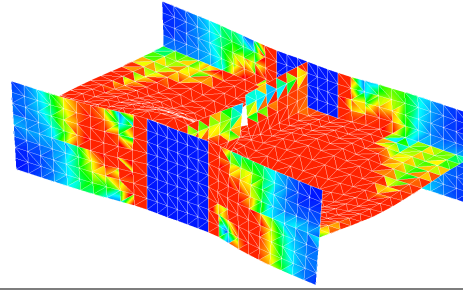
---



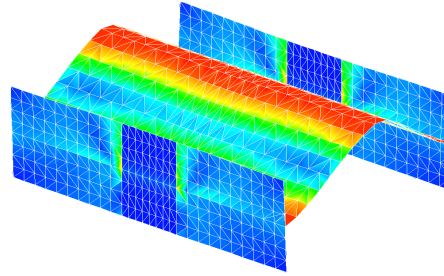
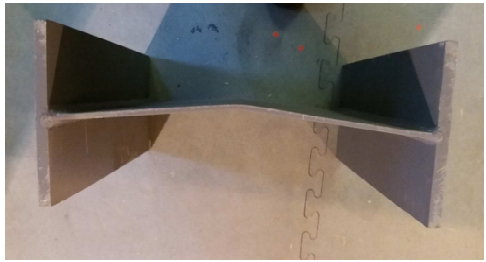
---

(e) Failure mode of 5.PC-H

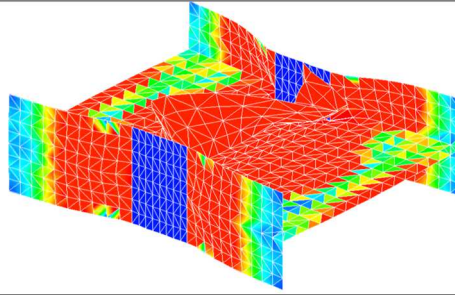
---



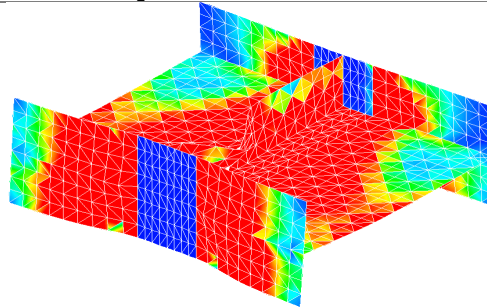
(f) Failure mode of 6.P2E-H



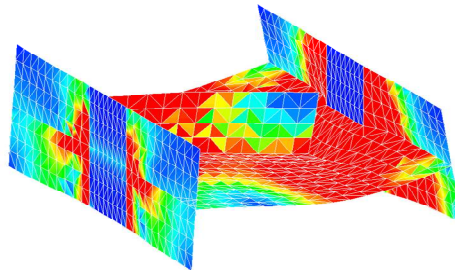
(g) Failure mode of 1.U-W<sub>λ1</sub>



(h) Failure mode of 2.FD-W<sub>λ2</sub>



(i) Failure mode of 3.FS-W<sub>λ2</sub>



(j) Failure mode of 4.PIE-W<sub>λ2</sub>

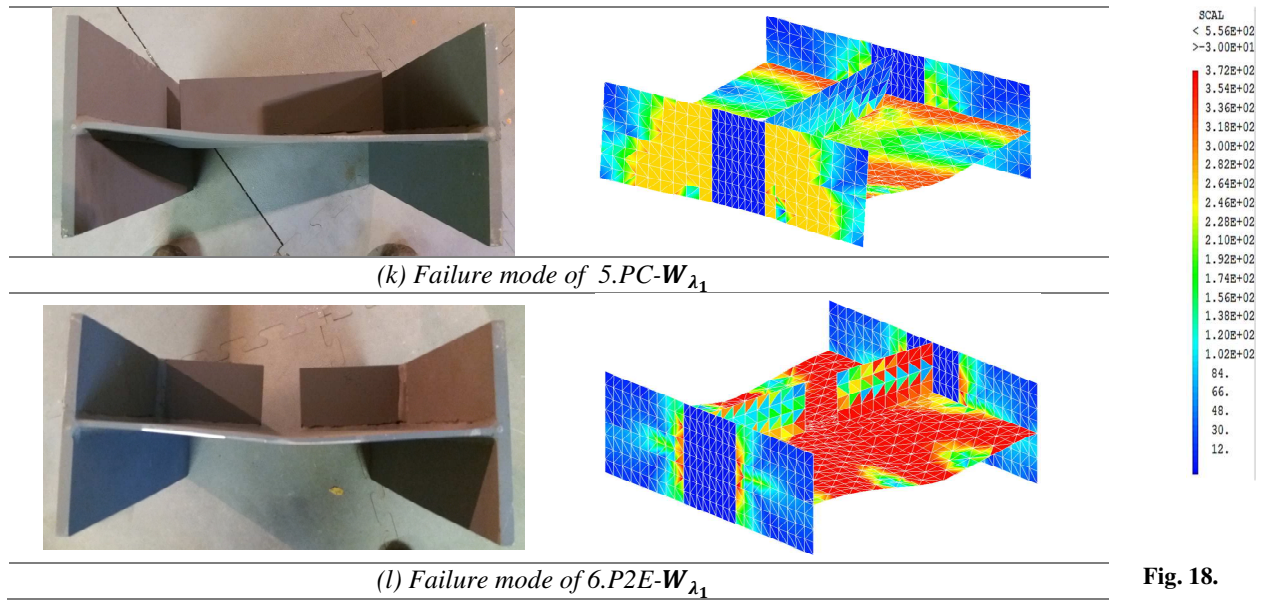


Fig. 18.

Failure modes (tests and finite element model)

#### 4. Analytical study

The analytical calculation can be done only for unstiffened and fully stiffened panels as no analytical formulation is available for party stiffened panels. The comparison is done between experimental ( $F_u$ , Test), numerical ( $F_u$ , FEM) and analytical ( $F_u$ , EN) maximum strength. The comparison for the specimens without stiffener (1.U-H and 1.U- $W_{\lambda_1}$ ) is shown on Table 7. The analytical calculations are based on equations (1 to 4) presented in the introduction.

Table 7: comparison between numerical, experimental, and analytical results (unstiffened panels)

$F_u$	Test	EN	DIFF ((EN-Test)/Test) (%)	FEM	DIFF ((EN-FEM)/FEM) (%)
1.U-H	478	394	-17.6	468.6	-15.9
1.U- $W_{\lambda_1}$	237	239.1	0.9	244.5	-2.2

The difference between experimental results and analytical formula is 17.6 % for the specimen 1.U-H, with analytical value lower than the experimental one. For the specimen 1.U- $W_{\lambda_1}$ , the difference is lower than 1 %.

For the specimens 3.FS-H, 3.FS- $W_{\lambda_2}$ , 2.FD-H and 2.FD- $W_{\lambda_2}$  equations (5 to 17) may be applied. Although, equation 5 is used to calculate the maximum resistance of plates with

stiffeners susceptible to undergoes flexural behavior under double opposite compression load, it may be a reference to compare with in these cases. The results are summarized in Table 8.

Table 8: comparison between FEM, EXP and TEST results (fully stiffened panels)

<b>Fu</b>	<b>Test</b>	<b>EN</b>	<b>DIFF ((EN-Test)/Test) (%)</b>	<b>FEM</b>	<b>DIFF ((EN-FEM)/FEM) (%)</b>
3.FS-H	876.8	857	-2.3	865.9	-1
3.FS- $W_{\lambda_2}$	1461	1358.8	-7	1482.1	-8.3
2.FD-H	1160.9	1149.1	-1.02	1183.3	-2.9
2.FD- $W_{\lambda_2}$	1768	1670	-5.5	1807.7	-7.6

The analytical formula is applied for single and double stiffened plates. The comparison between the results of the tests and the analytical formula proves that the analytical formula can be applied in the case of stiffened panels (the differences are lower than 10%).

## 5. Conclusions

In this paper, an experimental program of twelve I beam panels subjected to opposite patch loading is performed. The web panels are fully or partly stiffened with different positions of stiffeners. The experimental results are used to validate a finite element model based on shell elements. Maximum loads, load-displacement curves as well as the failure mode obtained from experimental and numerical studies are presented and compared. The model represents well the main parameters needed in the study (resistance and failure mode).

It was observed that the behavior of panel webs with transverse stiffeners under patch loading is strongly influenced by the dimensions and localization of the stiffeners. Besides, the resistances of the stiffened panels depend mainly on the unstiffened part of the web. In fact, similarities were observed between the partly stiffened panels with the same length of stiffeners even with different positions on the web. The fully stiffened panels undergo a torsional buckling either with single or double-sided stiffeners. The difference appears only in the value of the maximum load.

The maximum resistance of unstiffened or fully stiffened panels are calculated using the principles of EN1993-1-5 and their results compared with those of experimental and finite element. The calculated values predict well the real values of stiffened panels.

The experimental results completed by parametric study based on the finite element model, will be used to extend the analytical approach of Eurocode 3 to the partly stiffened panels. The development will be based on the maximum resistance followed by the stiffness. These parameters are useful for the semi-rigid analysis of the compressed part of steel connections.

### **Acknowledgments**

The authors would like to thank the company Gagne (Groupe Briand) from Puy-en-Velay for providing the specimens for the experimental program. They also thank the platform MSGC (Polytech Clermont-Ferrand) and its team of engineer and technicians (G. Godi, Ph. Phargeix, L. Phelipe) for the testing facilities.

### **6. References**

- [1] Eurocode 3 : Design of steel structures — Part 1-8 : Design of joints, 2010.
- [2] A.M. Girão Coelho, Numerical approach to the evaluation of the transformation parameter  $\beta$ , *J. Constr. Steel Res.* 133 (2017) 405–417. doi:10.1016/j.jcsr.2017.02.031.
- [3] C.J. Carter, S. Series, *Stiffening of Wide-Flange Columns at Moment Connections: Wind and Seismic Applications*, AISC Steel Des. Guid. Ser. (2003) 1–2.
- [4] F. Bijlaard, Eurocode 3, a basis for further development in joint design, *J. Constr. Steel Res.* 62 (2006) 1060–1067. doi:10.1016/j.jcsr.2006.06.012.
- [5] H. Tagawa, S. Gurel, Application of steel channels as stiffeners in bolted moment connections, *J. Constr. Steel Res.* 61 (2005) 1650–1671. doi:10.1016/j.jcsr.2005.04.004.

- [6] A. Abidelah, A. Bouchaïr, D.E. Kerdal, Experimental and analytical behavior of bolted end-plate connections with or without stiffeners, *J. Constr. Steel Res.* 76 (2012) 13–27. doi:10.1016/j.jcsr.2012.04.004.
- [7] Z. Al-Khatib, A. Bouchaïr, Analysis of a bolted T-stub strengthened by backing-plates with regard to Eurocode 3, *J. Constr. Steel Res.* 63 (2007) 1603–1615. doi:10.1016/j.jcsr.2007.01.012.
- [8] L.G. Johnson, Compression and tensile loading tests on joists with web stiffeners, *Br. Weld. J.* 6 (1959).
- [9] L.G. Johnson, Tests on welded connections between I-section beams and stanchions., *Br. Weld. J.* 6 (1959).
- [10] B. Bose, Design resistance of unstiffened column web subject to transverse compression in beam-to-column joints, *J. Constr. Steel Res.* 45 (1998) 1–15. doi:10.1016/S0143-974X(97)00065-5.
- [11] K. Bose, COLUMN WEBS IN STEEL BEAM-TO-COLUMN CONNEXIONS PART I-FORMULATION AND VERIFICATION, 2 (1972) 253–279.
- [12] L. Preserve, J.D. Graham A N Sherbourne R N Khabbaz C D Jensen, Welded interior beam-column connections, AISC Publication, 1959, Reprint No. 146 (59-7, 60-3), n.d. <http://preserve.lehigh.edu/engr-civil-environmental-fritz-lab-reports/1568>.
- [13] L. De Mita, V. Piluso, G. Rizzano, Theoretical and Experimental Analysis of Column Web in Compression, 2008.
- [14] A. Bergfelt, S.Lindgren, Local web crippling in thin-walled plate girders under concentrated loads, *Chalmers Univ. Technol. Publ. S74:* (1974).
- [15] S. Shimizu, A New Collapse Model for Patch-loaded Web Plates, 13 (1989) 61–73.

- [16] N. Europeenne, E. Norm, EUROPEAN STANDARD Eurocode 3-Design of steel structures-Part 1-5: Plated structural elements, 2006.
- [17] R. Chacón, E. Mirambell, E. Real, Transversally stiffened plate girders subjected to patch loading: Part 2. Additional numerical study and design proposal, *J. Constr. Steel Res.* 80 (2013) 492–504. doi:10.1016/j.jcsr.2012.06.001.
- [18] O. Lagerqvist, Patch Loading. Resistance of steel girders subjected to concentrated forces. Division of Steel Structures, Lulea Univ. Technol. Thesis,. (1994).
- [19] O. Mezghanni, J. Averseng, A. Bouchaïr, H. Smaoui, Behavior of beam web panel under opposite patch loading, *J. Constr. Steel Res.* 83 (2013) 51–61. doi:10.1016/j.jcsr.2012.12.018.
- [20] SteelConstruction.info, (n.d).  
[https://www.steelconstruction.info/The\\_Steel\\_Construction\\_Information\\_System](https://www.steelconstruction.info/The_Steel_Construction_Information_System).
- [21] A. Cevik, M. Tolga Göğüş, I.H. GüzelbeY, H. Filiz, A new formulation for longitudinally stiffened webs subjected to patch loading using stepwise regression method, *Adv. Eng. Softw.* 41 (2010) 611–618. doi:10.1016/j.advengsoft.2009.12.001.
- [22] C. Graciano, Strength of longitudinally stiffened Webs subjected to concentrated loading, *J. Struct. Eng.* 131 (2005) 268–278. doi:10.1061/(ASCE)0733-9445(2005)131:2(268).
- [23] B. Kövesdi, Patch loading resistance of slender plate girders with longitudinal stiffeners, *J. Constr. Steel Res.* 140 (2018) 237–246. doi:10.1016/j.jcsr.2017.10.031.
- [24] N. Loaiza, C. Graciano, R. Chacón, E. Casanova, 16.20: Influence of bearing length on the patch loading resistance of multiple longitudinally stiffened webs, *Ce/Papers.* 1 (2017) 4199–4204. doi:10.1002/cepa.477.

- [25] Q. Vu, V. Truong, G. Papazafeiropoulos, C. Graciano, S. Kim, Bend-buckling strength of steel plates with multiple longitudinal stiffeners, *J. Constr. Steel Res.* 158 (2019) 41–52. doi:10.1016/j.jcsr.2019.03.006.
- [26] C. Graciano, Patch loading resistance of longitudinally stiffened girders - A systematic review, *Thin-Walled Struct.* 95 (2015) 1–6. doi:10.1016/j.tws.2015.06.007.
- [27] American Association of State Highway and Transportation Officials, AASHTO LRFD Bridge Design Specifications, 2017.
- [28] K.N. Rahal, J.E. Harding, Transversely stiffened girder webs subjected to shear loading-part 1 : behaviour, (1990) 47–65.
- [29] S.C. Lee, M. Asce, C.H. Yoo, M. Asce, D.Y. Yoon, Behavior of Intermediate Transverse Stiffeners Attached on Web Panels, (2002) 337–345.
- [30] S.C. Lee, D.S. Lee, C.H. Yoo, Design of intermediate transverse stiffeners for shear web panels, *Eng. Struct.* 75 (2014) 27–38. doi:10.1016/j.engstruct.2014.05.037.
- [31] B.H. Choi, Y.J. Kang, C.H. Yoo, Stiffness requirements for transverse stiffeners of compression panels, *Eng. Struct.* 29 (2007) 2087–2096. doi:10.1016/j.engstruct.2006.11.002.
- [32] R. Chacón, J. Herrera, L. Fargier-Gabaldón, Improved design of transversally stiffened steel plate girders subjected to patch loading, *Eng. Struct.* 150 (2017) 774–785. doi:10.1016/j.engstruct.2017.07.086.
- [33] K. Le Tran, S. Et, D.E.L.A. Stabilit, oles courbes cylindriques en acier : applications aux ouvrages d ’ art Docteur de l ’ Universit ´, (2012).
- [34] Accueil | Cast3M, (n.d.). <http://www-cast3m.cea.fr/index.php>.

- [35] Y. Huang, B. Young, The art of coupon tests, *J. Constr. Steel Res.* 96 (2014) 159–175.  
doi:10.1016/j.jcsr.2014.01.010.